COMPOSITE FLOOR BEAMS WITH CONSTRAINED LAYER DAMPING: EXPERIMENTAL TESTS ON REDUCED SCALE MODELS

Carlos M. C. Renedo*, Wilson P. Ortega*, Iván M. Díaz* and Jaime H. G. Palacios†

* Department of Continuous Mechanics and Theory of Structures. ETSI Caminos, Canales y Puertos
Universidad Politécnica de Madrid
28040 Madrid, Spain
e-mail : carlos.martindelaconcha@upm.es
ORCID : 0000-0003-1014-0878

† Department of Hydraulics, Energy and Environmental Engineering. ETSI Caminos, Canales y Puertos
Universidad Politécnica de Madrid
28040 Madrid, Spain

Abstract. Vibration Serviceability Limit State due to human-induced vibrations is an important requirement that increasingly influences the sizing of current long-span floors. Usually, structural designers tend to overcome this issue by stiffening the floor to avoid any low-frequency response in resonance with human footfalls. An alternative solution to this one consist of increasing the floor's damping to enhance its dynamic performance.

This paper experimentally studies the effectiveness of a Constrained Layer Damping (CLD) treatment applied along the whole length of a typical composite floor beam. The aim of the paper is to quantify the additional damping ratio provided by this damping technique. To reduce the economical and time effort involved in a Full-scale experimental campaign, two reduced-scale models (RSMs) were developed with and without any CLD treatment. Those models were designed to exhibit the same amount of extra damping ratio when treated with the same CLD configuration to be used in Full-scale specimens. Once the RSMs were designed and built, free-response tests were performed to derive their natural frequencies and the relation between their damping ratio and the vibration amplitude.

Key words: Constrained Layer Damping, Floor vibration, Viscoelastic materials, Experimentation, Composite structures.

1 INTRODUCTION

Nowadays, architectural trends in office buildings demand open-plan spaces that minimize the presence of non-structural elements (avoiding vertical partitions, heavy furniture, paper cabinets, etc.) [1]. In this context, steel-concrete composite floor systems have become a common structural solution for these spaces. The use of stronger steel beams reduces the floor's weight and increases its strength, which enables it to be a competitive solution especially for long spans between 8 and 15 m [2]. Typically, the structural design of floor structures has been governed by the Deformation Serviceability Limit State, however, since these modern and long-span floors became a widespread solution, their dynamic performance begun to worry structural designers [3].

As a result of all mentioned, current open-plan office floors have less self-weight, less dead loads, and less inherent damping, and therefore, their performance against dynamic

loads (such as those induced by humans at walking) has deteriorated. Modern floors are "livelier" than in the past. Furthermore, the tolerance vibration levels related to offices are quite restrictive (around 0.04 m/s^2), as they are classified as calm spaces. All this has led to consider the Vibration Serviceability Limit State (VSLS) as an important requirement that these floors must fulfil to be functional [4].

Most of the guidelines focused on assessing the VSLS of floors [4],[5],[6] usually classify them into two types according to their fundamental natural frequency: low frequency floors (LFFs) and high-frequency floors (HFFs) by setting the limit at 10 Hz. This approach is based on floors' dynamic response to human-induced vibration. LFF tend to develop remarkable resonant responses with higher harmonics of the human load (between 5 and 8 Hz), whereas HFF responses are predominantly non-resonant presenting a peak in the transient regime. Currently, many long-span composite floors tend to be LFF and thus, VSLS check is even more crucial at the design stage [7].

When facing the design of a "lively" LFF, structural engineers usually tend to overcome the VSLS through enlarging the steel members, and thus, increasing the system stiffness until the dynamic response predicted by a footfall analysis is below the required tolerance limit [8]. This implies to oversize the floor in terms of strength, decreasing a lot its section utilization. This approach is not beneficial in terms of CO^2 credentials, even less so when considering that floors may represent up to the 30% of the embodied carbon footprint of a steel framed building [9].

The dynamic performance of a LFF may also be considerably improved through increasing its damping, as this parameter is inversely proportional to the steady-state response of the system. There are different technologies that can be implemented for that, such as for example inertial dampers [10] (commonly known as Tuned Mass Dampers or TMDs), viscous dampers or active solutions that mitigate the vibration in real time [11]. In addition to these, in 2006 ARUP came up with a new damping solution called "Resotec" that integrated Constrained Layer Damping (CLD) into composite floors. This system is based on the use of a thin layer of high-damping viscoelastic (VE) material (around 1 mm thick) comprised between two thin steel sheets. This 3-layer element is integrated between the concrete slab and the steel member of a composite beam for a certain proportion of its length near the support. Along this portion, the steel beam and the concrete slab are disconnected to shear as depicted in Figure 1. When the floor vibrates in a bending mode, the slab slips with respect to the steel beam and the intermediate VE layer develops a shear hysteretic behaviour in which mechanical energy is dissipated [12].

Willford et al. provided the description, a brief analysis and a full-scale experimentation of "Resotec" for a composite beam specimen of 12 m span. They reported a 2% damping ratio increase for a "Resotec" application along the 50% of the specimen length (50%-CLD). The authors consider that despite the results obtained by Willford et al. are encouraging, the research community has not focused enough attention on this topic. As a consequence, the results provided in [12] are considered to be limited and insufficiently contrasted.

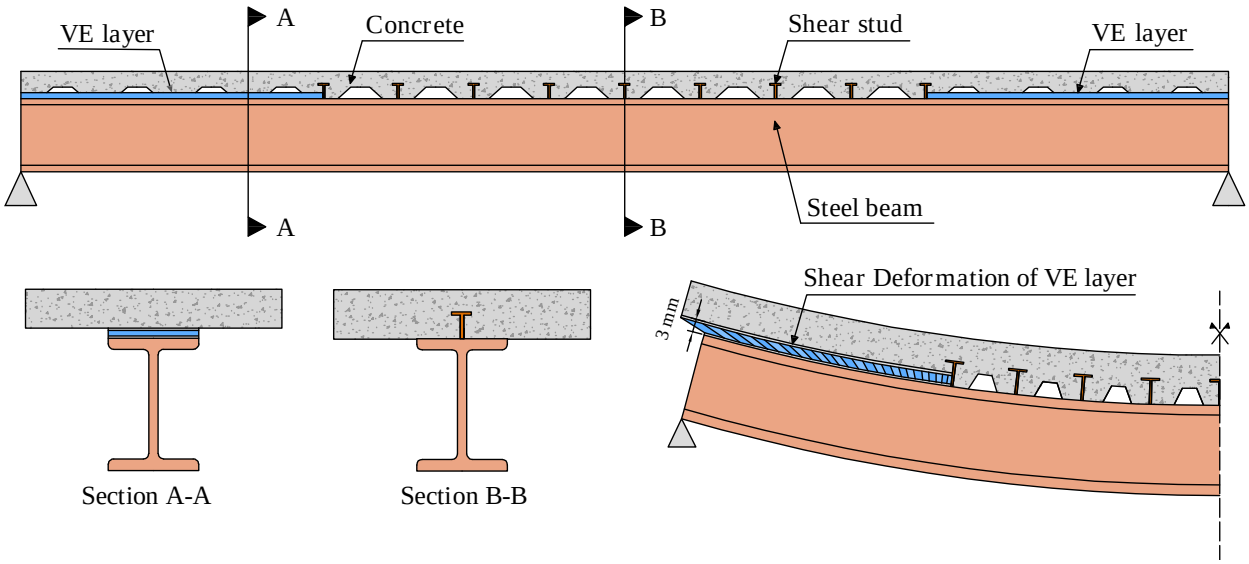

Figure 1 CLD treatment integrated into a composite floor beam for 50 % of its length.

This paper is focused on the development of experimental tests to validate the use of CLD systems in LFFs. Since the construction of a full-scale long-span composite floor prototype is costly and difficult, reduced scale models have been developed by means of scaling laws. The study is based on two reduced-scale composite specimens of 3,60 m long. The first one called 0%-CLD does not incorporate any damping treatment, so the concrete slab and the steel beam are connected by means of studs. The second one called 100%-CLD incorporates CLD treatment along its entire length.

The remainder of this paper is organized as follows: In Section 2 the mechanical behaviour of a VE material is described. Section 3 explains the different techniques to increase the damping through integrating VE materials within a structural matrix. Section 4 exposes the development of the reduced scales models employed in the paper. Section 5 describes the experimental test performed and Section 6 provides the results obtained. Finally, Section 7 outlines some conclusions.

2 MECHANICAL PROPERTIES OF VE MATERIALS

The mechanical properties of VE materials are time-dependent. These properties are mainly characterized by two rheological phenomena: relaxation and creep [13]. Indeed, this fact enables to analyze the VE mechanical behavior in the frequency domain thanks to the Fourier transform. This means to study the response of a VE material to harmonic excitations (such as a cyclic stress or a harmonic imposed strain). This approach results in a stress-strain relation defined by a Frequency Response Function (FRF) in the $j\omega$ domain. When performing this study for shear stresses and strains this FRF is defined as follows:

$$\frac{\tau(j\omega)}{\gamma(j\omega)} = G^*(j\omega) = G'(\omega)(1+j\eta(\omega)) \quad (1)$$

$$G^*(j\omega) = G'(\omega) + jG''(\omega) \quad (2)$$

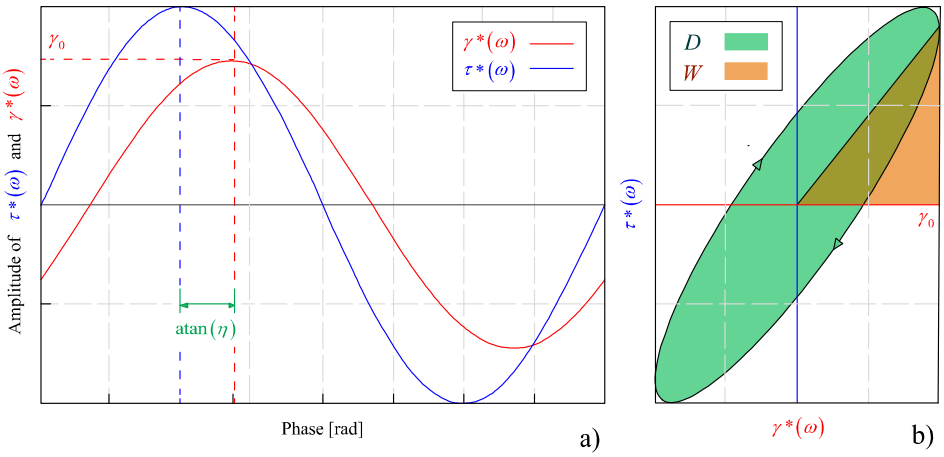

Figure 2 Shear stress and shear strain relation for a certain frequency

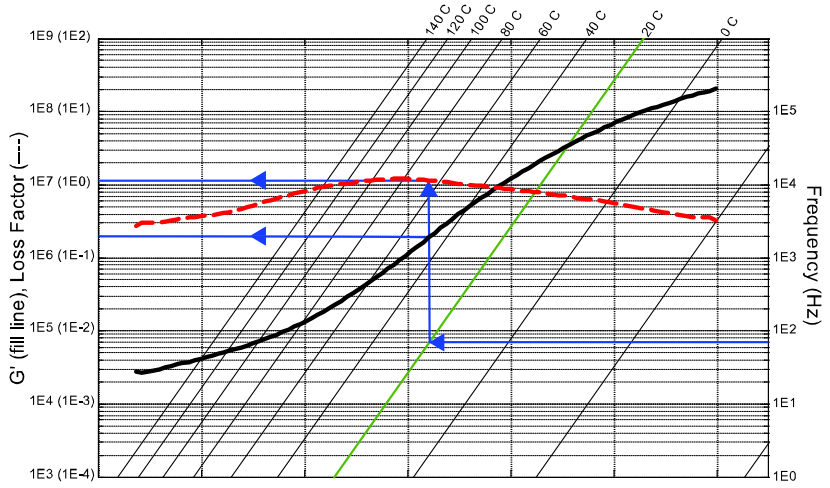

Figure 3 Nomogram of HIP2, the VE material used for the experimental tests presented in the paper [15].

where $G^*(j\omega)$ corresponds to the complex FRF usually called complex shear modulus. $G'(\omega)$ is its real part referred as the 'storage modulus' due to it represents the elastic component of the VE behavior. $G''(\omega)$ is the so called 'dissipation modulus' as it plays the role of the viscous component. Additionally, $\eta(\omega)$ represents the phase of this FRF and it is named 'loss factor'. The higher the phase between strain and stress the higher the energy dissipated per vibration cycle as depicted in Figure 2. The amplitude or gain of this FRF may be computed as follows:

$$|G^*(\omega)| = \sqrt{\left(G'(\omega)\right)^2 + \left(G''(\omega)\right)^2} \qquad (3)$$

Additionally, VE mechanical behavior is also influenced by temperature. In fact, an analogy can be stablished between temperature and frequency dependent properties, the so called 'Time-Temperature equivalence'. This enables to sum up the mechanical properties of a certain VE material in a single abacus called 'Nomogram' [14]. Figure 3 depicts the correct way of reading a Nomogram for a given temperature and frequency, the provided is from the HIP2 from (Heathcote

Industrial Plastics) material used in this paper [15].

DAMPING INCREASE WITH LAYERS OF VE MATERIAL

VE materials have been mainly used in aircraft and mechanical engineering to mitigate undesired vibrations. Their use was then extended to civil engineering in the form of the well-known VE dampers. These devices concentrated their action into a single structural point, where the VE material was located acquiring a great shear strain. They have been widely used for cancelling seismic and wind-induced vibrations as Figure 4 depicts [16].

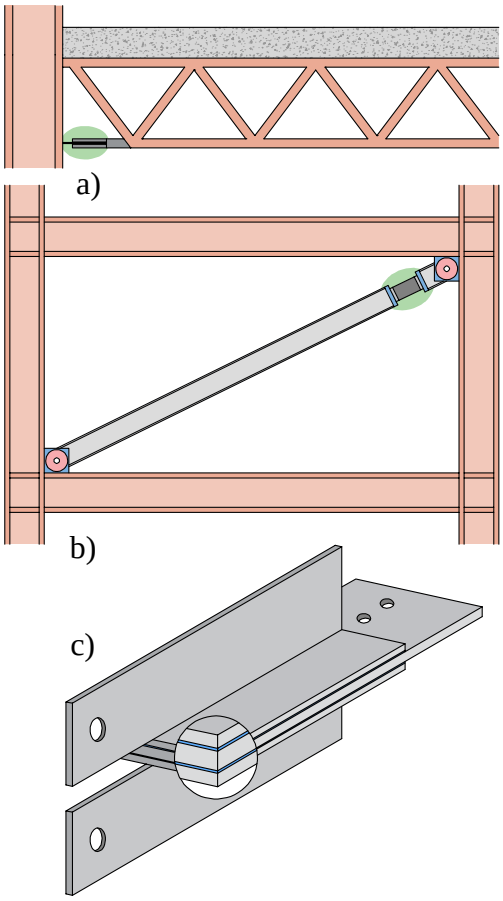

Figure 4 VE Dampers (c) applied in high rise buildings to mitigate wind-induced (a) and seismic vibrations (b) [16].

In addition to this damping technology, VE materials have been successfully applied as thin layers or 'tapes' glued to a bending-vibrant surface on a wide variety of mechanical systems [17]. In these cases, they are intended to dissipate energy through normal or shear stress loading cycles. Hence, two types of treatments may be differentiated:

Unconstrained Layer Damping (ULD): consists in attaching a VE layer to an eccentric surface of the structural element to be treated. ULD enables additional energy dissipation through extensional hysteresis of the VE tape. The additional damping achieved with this technique is usually small (Figure 5.a).

Constrained Layer Damping (CLD): consists in constraining a layer of VE material between two bending elements. In this case the layer must be located as closer as possible to the sectional centroid of the element to be treated, as the energy dissipation is achieved through a shear hysteresis. This treatment usually provides greater damping improvements than the ULD. It is important to note that in CLD treatments there exists an optimum geometry (thickness and width) of the VE layer that provides a maximum damping increase (Figure 5.b).

Both damping treatments are depicted in Figure 5 which also includes the rules of thumb for efficiently designing them. As mentioned before, this paper is about the integration of a CLD treatment into composite floor systems.

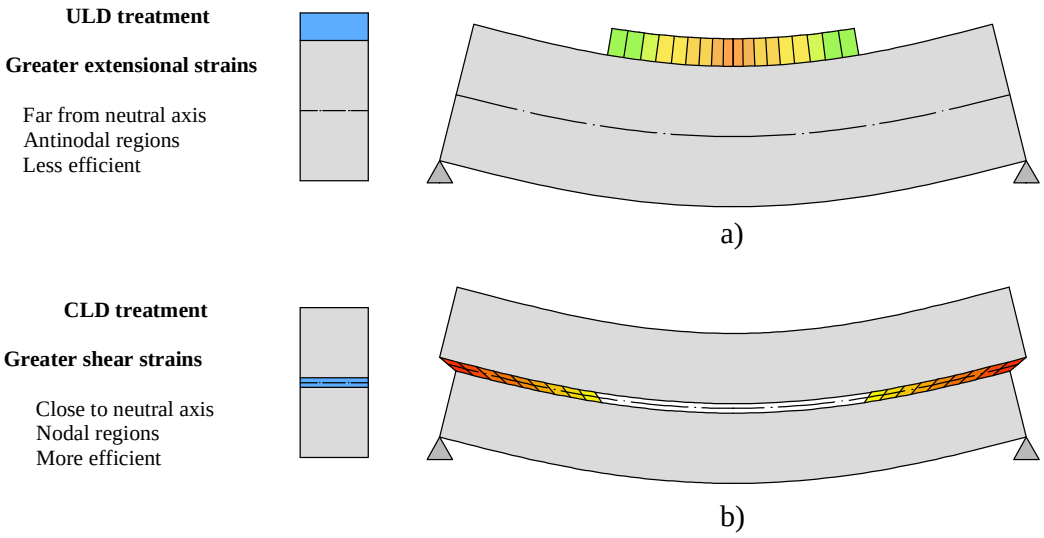

Figure 5 ULD (a) and CLD (b) damping treatments [17].

4 DEVELOPMENT OF REDUCED SCALE MODELS

From now on, the text will refer to two different concepts, "Full-scale model" (FSM) which refers to the system for which predictions have been made, and "Reduced-Scale model" (RSM) which refers to the model itself that has been used to reproduce the first one.

The FSM studied is a long-span composite floor beam of 12 m span. The objective of the paper is to know the additional damping ratio provided by a 100%-CLD treatment applied along the whole length of the studied beam. Thus, ideally, two FSMs would be tested with and without CLD. The beam without any damping treatment would be expected to be stiffer, hence its fundamental natural frequency would be higher, as the concrete slab would be connected to the steel profile through shear studs, however, its damping ratio would be considerably lower.

The RSM proposed has been intended to provide the same amount of additional damping ratio when treating it with the same CLD configuration that would be applied to the FSM. This has enabled to perform the same experimental test as those that would have been performed in the FSM but without so much time, economical and facility resources.

The conceptual design of the RSM was the same as the FSM's one: a composite beam consisting in a concrete slab and a steel profile beam. This decision was adopted for the RSM to be representative, thus, for preserving certain realism. Both concrete and steel mechanical properties were considered identical for FSM and RSM.

The following subsection describes the methodology used to obtain the final geometry of the equivalent RSM.

4.1 Methodology adopted to compute the RSM adequate dimensions

The following methodology is based on an analytical solution developed by Mead for the study of simply-supported beams with 100%-CLD treatment [17]. This solution enables knowing the extra damping ratio provided by the CLD treatment and it is based on two dimensionless parameters. These can be computed from the beam's mechanical and geometrical properties (outlined in Figure 6.a).

The 'geometric parameter' Y which represents the loss of beam's bending resistance when the 100%-CLD treatment is applied,

$$Y = \frac{d_{321}^2}{(EI_t)}\left[\frac{E_1A_1E_3A_3}{E_1A_1+E_3A_3}\right], \qquad (4)$$

and the 'modified shear parameter' g_i that indicates the shear stiffness of the constrained VE layer for a given vibration mode of the beam,

$$g_i = \frac{G'_2\, b_2 L_b^2}{i^2\pi^2 h_2}\left[\frac{1}{E_1A_1}+\frac{1}{E_3A_3}\right], \qquad (5)$$

where, E_1, A_1 and I_1 are the Young modulus, the area and the moment of inertia of the steel profile and E_3, A_3 and I_3 are the same for the concrete slab, d_{321} is the distance between the sectional centroids of the concrete slab and steel beam, EI_t is the beam's bending stiffness when the slab and the profile are disconnected to shear and bend as independent elements, G'_2 is the 'storage modulus' of the VE material, b_2 and h_2 are the width and the height of the VE layer, respectively, i indicates the vibration mode to be analyzed and L_b the length of the beam.

Mead's solution allows computing the additional modal damping ratio of the treated beam as a function of Y, g_i and η_2 (the loss factor of the VE material used) as follows:

$$\xi_i \approx \frac{g_i\eta_2 Y}{2\left(1+g_i(2+Y)+g_i^2\left(1+\eta_2^2\right)(1+Y)\right)} \qquad (6)$$

As the formulation provided by Mead is dimensionless, it can be used to develop some scaling laws for obtaining the adequate geometry of the RSM. Those scaling equations need to be intended to achieve a reasonable similarity between the FSM and the RSM. Therefore, since the damping increment provided by the CLD treatment is the fundamental parameter to be studied in this paper, the first scaling equation used was the following one:

$$\xi_{1FS} = \xi_{1RS} \qquad (7)$$

where ξ_{1RS} and ξ_{1FS} are the extra damping ratio of the RSM and of the FSM respectively, and they need to be equal.

To achieve a higher degree of similarity, a second scaling equation was imposed. The aim of this second condition was to make a RSM with the same loss of bending resistance when the CLD would be applied. Thus, it was expressed as follows:

$$Y_{RS} = Y_{FS} \qquad (8)$$

where Y_{RS} and Y_{FS} are the 'geometric parameter' for the RSM and FSM, respectively.

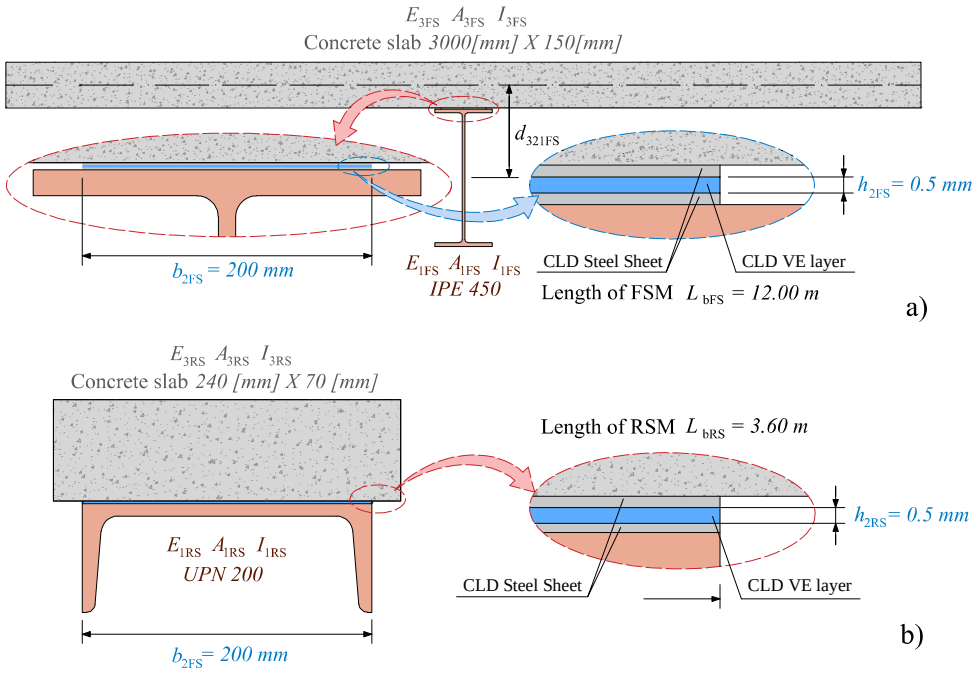

Figure 6 FSM (a) and RSM (b) geometry and CLD details.

Finally, the following equations were imposed to achieve that the CLD configuration and the mechanical properties of the materials used were the same for RSM and FSM.

$$h_{2RS} = h_{2FS}, \tag{9}$$

$$b_{2RS} = b_{2FS}, \tag{10}$$

$$E_{1RS} = E_{1FS}, \tag{11}$$

$$E_{3RS} = E_{3FS}. \tag{12}$$

Some additional constraints were imposed on the RSM design. First, its length (L_{bRS}) should be lower than 4 m, to minimize its impact on the laboratory,

$$L_{bRS} < 4m. \tag{13}$$

Second, the fundamental natural frequency of the RSM with 0% CLD ($f_{1RS-0\%}$) should be lower than 20 Hz, to ease its testing with an electrodynamic shaker:

$$f_{1RS-0\%} < 20Hz \tag{14}$$

Additionally, the mechanical properties of the VE layer need to be considered in the design. These depend on frequency and on temperature. Hence, a certain temperature should be chosen for computing the equivalent RSM. The temperature at which RSM and FSM are equivalent was decided to be 20º C. For the experimental test, this value was assured by means of a thermostat. In addition, the VE mechanical properties also rely on frequency. The fundamental natural frequency of the specimen must be used to compute them as the additional modal damping ratio to be studied corresponds to a fundamental bending mode. It should be noted that none scaling condition was imposed with respect to $f_{1RS-100\%}$.

Consequently, the resulting $f_{1RS-100\%}$ is considerably higher than $f_{1FS-100\%}$. This means that the VE properties of the RSM (G'_{2RS} and η_{2RS}) are different to those of the FSM (G'_{2FS} and η_{2FS}). This fact could not be avoided as L_{bRS} needed to achieve a frequency value identical to $f_{1FS-100\%}$ would have been much higher than 4 m.

Mead also provided an approximated way of computing the natural frequency of a 100%-CLD beam according to the following equation:

$$f_{i-100\%} = \sqrt{\frac{i^4\pi^2\left(EI_t\right)}{4m_tL_b^4}\left[1+\frac{g^*Y}{\left(\frac{i\pi}{L_b}\right)^2+g^*}\right]}, \quad (15)$$

where m_t is the mass per unit of length of the beam and g^* is the so called 'shear parameter' computed as follows:

$$g^* = \frac{G_2'b_2}{h_2}\left[\frac{1}{E_1A_1}+\frac{1}{E_3A_3}\right] \quad (16)$$

The determination of the natural frequency of a VE damped structure is a convergent iterative process in which the properties of the VE material vary and at the same time modify the natural frequency of the overall system. This iterative procedure is shown in Figure 7 and it is used in this paper.

4.2 FSM to be reproduced, geometry and mechanical properties

The FSM chosen is intended to be a typical composite floor beam used for long-spans. It consists in a 12 m span beam composed by an IPE 450 S355 steel profile and a concrete slab of 3 m width by 0.15 m height as the one shown in Figure 6.a. The concrete Young modulus chosen is 30 GPa and the steel modulus is 210 GPa. The width of the integrated CLD is 200 mm and the height of its VE layer is 0.5 mm. Furthermore, the thickness of the constraining steel plates belonging to the CLD is also 0.5 mm.

The VE material used is the HIP2, a polymer manufactured by Heathcote Industrial Plastics whose properties are defined in the nomogram depicted Figure 3. The predicted natural frequencies and additional damping of the FSM are the following ones:

Table 1 Dynamic properties of the FSM.

$f_{1FS-0\%}$ [Hz]	$f_{1FS-100\%}$ [Hz]	ξ_{1FS} [%]
4.86	4.34	7.30

4.3 RSM designed, geometry and mechanical properties

To design the RSM, the following strategy was adopted. First, four varying geometrical parameters were defined for combining them and achieve and adequate design: a steel profile ranging between the UPN 140 and the

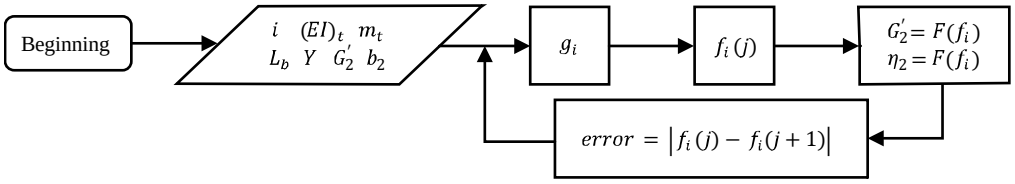

Figure 7 Convergent iterative process for determining the natural frequency of a VE damped structure.

Table 2 Detailed dynamic properties estimated for the RSMs developed.

Beam [Prof]	bc_{RS} x hc_{RS} [mm^2]	L_{bRS} [m]	Y_{RS} [-]	g_{1RS} [-]	G'_{2RS} [Mpa]	η_{2RS} [-]	$f_{1RS-0\%}$ [Hz]	$f_{1RS-100\%}$ [Hz]	ξ_{1RS} [%]
UPN 200	240 X 70	3.60	1.64	1.38	0.80	1.01	18.04	15.10	7.30

UPN 240, the width of the concrete slab (bc_{RS}) defined between 0.2 and 0.4 m, the slab height (hc_{RS}) limited between 0.05 m and 0.15 m due to constructive reasons, and the beam span (L_{bRS}) ranged from 1 to 4 m. Those combinations of UPN, bc_{RS}, hc_{RS} and L_{bRS} complying with the scaling laws exposed from Equations (7) to (12) were obtained by performing an iterative computation. The mechanical properties of the steel and the concrete were assumed to be identical to those used in the FSM. Finally, those successful geometrical layouts were filtered according to the natural frequency constrain exposed in Equations (14). From among the finalist equivalent geometries the authors chose the one with a lower natural frequency and a feasible concrete height from a constructive point of view.

The final RSM obtained by means of the described procedure is presented in Figure 6 and its estimated dynamic properties are outlined in Table 2. It consists in a 3.60 m span composite beam with an UPN 200 steel profile and a small concrete slab of 0.24 m width by 0.07 m height. The geometry of the CLD treatment used for the RMS is identical to the one assumed in the FSM (Figure 6.b).

5 EXPERIMENTAL TESTS

5.1 Experimental tests performed

In the present study, free vibration response tests of the RSMs against an impulsive load provided using an elastic-tip hammer were performed. Impulsive loads were located next to the mid-span section. An accelerometer was placed at mid span to obtain the beam's free response in terms of acceleration. The transducer used was a PCB 393B12 accelerometer with a sensitivity of 1V/m/s^2 and a measurement range of ±5 m/s^2. The measurements were acquired using a NI CompactRIO 9066 with a NI 9234 acquisition module for reading IEPE Voltage signals. A sampling frequency of 1000 Hz was used.

Three experimental tests were developed, one for 0%-CLD beam, and two tests for the 100%-CLD mode (a first one at 10º C and a second one at 20 ºC). These free vibration tests were performed hitting the models with the hammer several times during a single measurement that lasted 200 seconds. After each hit the beam was left vibrating freely until the vibration was completely damped. Once recorded, the signal was divided into several free-decay 'subtests' which were analyzed independently.

5.2 Experimental data processing

Two types of data processing were performed for each free-decaying 'subtest'. First, the damping ratio of the studied

specimen was computed as a function of the vibration amplitude. For that, the damping ratio was estimated from the logarithmic decrement at each vibration cycle for a given number of subsequent vibration cycles, as follows:

$$\xi \approx \frac{1}{2\pi N} \ln\left[\frac{u_i}{u_{i+N}}\right], \qquad (17)$$

where N is the number of vibration cycles chosen to compute the logarithmic decrement (3 in this paper), u_i is the amplitude of vibration the first vibration cycle and u_{i+N} the amplitude of the last cycle.

Secondly, the frequency spectrum for each 'subtest' was derived by means of a Fast Fourier Transform. The peak-picking method was used to determine the natural frequency of the studied specimen. Finally, all the computed values were averaged to determine the final value of the fundamental natural frequency.

6 RESULTS

The results of the experimental natural frequencies for the RSMs are given in Table 3. Figure 8 provides the results related to the damping ratio of the models. Polynomial tendencies have been included in this Figure.

In terms of natural frequencies, the experimental results are quite similar to those predicted. The lower natural frequency of the 0%-CLD specimen is probably due to the concrete-steel shear connection which is not perfectly rigid as it was assumed. In addition, for the 100%-CLD beam it can be observed a decrease in the natural frequency as the temperature increases, which seems to be logical as the shear modulus of a VE material tend decrease with temperature.

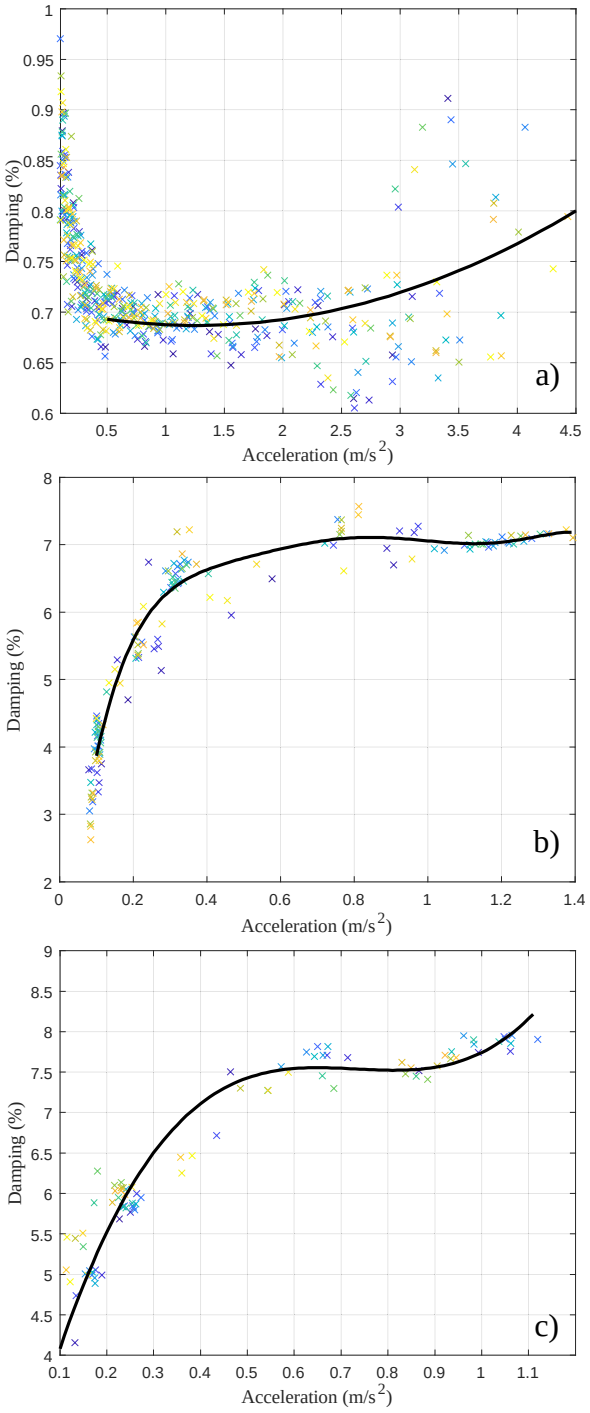

Figure 8 Damping ratio against acceleration for the three studied RSMs. a) 0%-CLD b) 100%-CLD at 10ºC and c) 100%-CLD at 20ºC.

Results provided in Figure 8 provide clear information about the RSM behavior in relation to damping ratio. First, for the 100%-CLD model, the higher the amplitude of vibration the higher the damping ratio as usually happens. For the 0%-CLD beam the relation between damping and amplitude is not so clear.

For higher accelerations (above 0.2 m/s^2), the VE layer seems to be 'switched on' and consequently dissipates additional energy through shear hysteresis. For lower amplitudes, this dissipating mechanism does not seem to be activated, and thus the damping ratio decreases. This might suggest that HIP2 mechanical properties could also depend on the amplitude of the excitation. Further characterization of this material would be needed to confirm this. For higher amplitudes, the experimental results match well with the additional damping ratio predicted (around 7%).

Table 3 Experimental frequencies of the RSMs tested.

$f_{1RS-0\%}$ [Hz]	$f_{1RS-100\%}$ at 10ºC [Hz]	$f_{1RS-100\%}$ at 20ºC [Hz]
16.70	15.43	15.00

7 CONCLUSIONS

This paper has presented an experimental study related to composite floor beams with integrated CLD. The damping treatment studied is like the one proposed by Willford et al. in 2006, in which a thin VE layer is constrained between the concrete slab and the steel profile of a composite beam. The paper aims to experimentally quantify the additional damping ratio provided by a CLD treatment applied along the whole length of a floor beam (100%-CLD).

To reduce the amount of economical, time and facility resources to be involved in the experimental campaign, the authors decided to develop two RSMs with and without CLD treatment. These models reproduce the dynamic behavior of a Full-Scale composite beam (named as FSM) of 12 m span. They were designed to achieve the same amount of additional damping ratio as the FSM with the same CLD configuration. The proposed scaling laws to design the RSM geometry are based on a dimensionless analytical solution provided by Mead for 100%-CLD beams.

Free-decay test have been performed by means of hammer impacts and the measured acceleration responses have been analyzed. The fundamental natural frequencies of the RSMs and the relation between their damping ratios and the amplitude of vibration have been derived. Finally, as a conclusion, it can be said that the results obtained corroborate the validity of Mead's dimensionless solution and thus, the scaling procedure developed in the paper. Therefore, it can be concluded that a 100%-CLD treatment applied to a composite floor beam (like the one proposed in this paper) may provide a remarkable increase in the damping ratio.

8 AWKNOWLEDGEMENTS

The authors acknowledge the Spanish Ministry of Science, Innovation and Universities through the project SEED-SD (RTI2018-099639-B-I00). Carlos M. C. Renedo would like to thank Universidad Politécnica de Madrid for the financial support through a PhD research grant.

REFERENCES

[1] A. Ebrahimpour and R. L. Sack, "A review of vibration serviceability criteria for floor structures," *Comput. Struct.*, vol. 83, no. 28-30 SPEC. ISS., pp. 2488–2494, 2005, doi: 10.1016/j.compstruc.2005.03.023.

[2] Ove Arup and Partners, "Structural Scheme Design Guide," 2006.

[3] W. I. Simms and A. F. Hughes, *Composite design of steel framed buildings*, 1st ed. Ascot: Steel Concrete Institute, 2011.

[4] T. M. Murray, D. E. Allen, E. E. Ungar, and D. B. Davis, *AISC Steel Design Guide 11. Vibrations of Steel-Framed Structural Systems Due to Human Activity*, Second. AISC, 2016.

[5] A. L. Smith, S. J. Hicks, and P. J. Devine, *Design of Floors for Vibration : (Revised Edition , February 2009)*, Second. Ascot: SCI, 2009.

[6] M. R. Willford and P. Young, *A Design Guide for Footfall Induced Vibration of Structures*. Surrey: The Concrete Society, 2006.

[7] Z. O. Muhammad and P. Reynolds, "Vibration Serviceability of Building Floors: Performance Evaluation of Contemporary Design Guidelines," *J. Perform. Constr. Facil.*, vol. 33, no. 2, pp. 1–17, 2019, doi: 10.1061/(ASCE)CF.1943-5509.0001280.

[8] J. J. Connor, *Introduction To Structural Motion Control*, First. Boston: Prentice Hall, 2002.

[9] V. J. L. Gan, C. M. Chan, K. T. Tse, I. M. C. Lo, and J. C. P. Cheng, "A comparative analysis of embodied carbon in high-rise buildings regarding different design parameters," *J. Clean. Prod.*, vol. 161, pp. 663–675, 2017, doi: 10.1016/j.jclepro.2017.05.156.

[10] T. H. Nguyen, I. Saidi, E. F. Gad, J. L. Wilson, and N. Haritos, "Performance of distributed multiple viscoelastic tuned mass dampers for floor vibration applications," *Adv. Struct. Eng.*, vol. 15, no. 3, pp. 547–562, 2012, doi: 10.1260/1369-4332.15.3.547.

[11] C. Camacho-Gómez, X. Wang, E. Pereira, I. M. Díaz, and S. Salcedo-Sanz, "Active vibration control design using the Coral Reefs Optimization with Substrate Layer algorithm," *Eng. Struct.*, vol. 157, no. November 2017, pp. 14–26, 2018, doi: 10.1016/j.engstruct.2017.12.002.

[12] M. Willford, P. Young, and W. H. Algaard, "A constrained layer damping system for composite floors," *Struct. Eng.*, vol. 84, no. 4, pp. 31–38, 2006.

[13] A. M. Baz, "Active and Passive Vibration Damping," in *Active and Passive Vibration Damping*, Wiley, Ed. Chichester, West Sussex, England: John Wiley and Sons, 2019.

[14] D. I. G. Jones, "Shock and Vibration Handbook," in *Shock and Vibration Handbook*, Fifth Edit., McGRAWHILL, Ed. New York: McGRAWHILL, 2002.

[15] H. I. Plastics, "HIP2 Material Properties," Staffordshire, 2020.

[16] B. Samali and K. C. S. Kwok, "Use of viscoelastic dampers in reducing wind- and earthquake-induced motion of building structures," *Eng. Struct.*, vol. 17, no. 9, pp. 639–654, 1995, doi: 10.1016/0141-0296(95)00034-5.

[17] D. J. Mead, "Passive Vibration Control," in *Passive Vibration Control*, John Wiley & Sons, Ed. Southampton: John Wiley & Sons, 2000, p. 591.